Supplementary Material

Marine anoxia initiates giant sulfur-bacteria mat proliferation and associated changes in benthic nitrogen, sulfur, and iron cycling in the Santa Barbara Basin, California Borderland

David J. Yousavich[1*], De'Marcus Robinson[2], Xuefeng Peng[3], Sebastian J. E. Krause[1,4], Frank Wenzhoefer[5,6,7], Felix Janβen[4,5], Na Liu[8], Jonathan Tarn[8], Frank Kinnaman[8], Dave Valentine[8], Tina Treude[1,2*]

[1]Department of Earth, Planetary, and Space Sciences, University of California Los Angeles, 595 Charles E. Young Drive East, Los Angeles, CA 90095, USA

[2]Department of Atmospheric and Oceanic Sciences, University of California Los Angeles, Math Science Building, 520 Portola Plaza, Los Angeles, CA 90095, USA

[3]School of Earth, Ocean, and Environment, University of South Carolina, 701 Sumter Street, EWS 617, Columbia, SC 29208, USA

[4]Earth Research Institute, 6832 Ellison Hall, University of California Santa Barbara, Ca 93106-3060

[5]HGF-MPG Joint Research Group for Deep-Sea Ecology and Technology, Alfred-Wegener-Institute, Helmholtz-Center for Polar and Marine Research, Am Handelshafen 12, 27570 Bremerhaven, Germany

[6]Max Planck Institute for Marine Microbiology, Celsiusstrasse 1, 28359 Bremen, Germany

[7]Department of Biology, DIAS, Nordcee and HADAL Centres, University of Southern Denmark, 5230 Odense M, Denmark

[8]Department of Earth Science and Marine Science Institute, University of California, Santa Barbara, CA 93106, USA

Correspondence: David Yousavich (yousavdj@ucla.edu), Tina Treude (ttreude@g.ucla.edu)

Supplemental Table 1: Porewater nitrite concentrations taken from sediment cores at SDRO and SDT3-A. Nitrite was below detection in sediment cores for all other stations; n.d. = not determined.

Sediment Depth [cm]	SDRO [NO_2^-] [$\mu mol\ L^{-1}$]	SDT3A [NO_2^-] [$\mu mol\ L^{-1}$]
-1	1.1	0.0
0.5	36.6	5.2
1.5	1.4	1.7
2.5	1.1	0.7
3.5	1.1	0.0
4.5	1.2	0.0
5.5	0.0	0.0
6.5	6.1	0.0
7.5	4.3	0.0
8.5	0.0	0.0
9.5	0.0	0.0
11	0.0	n.d.
13	0.0	n.d.
15	0.0	0.0
17	0.0	0.0
19	n.d.	0.0
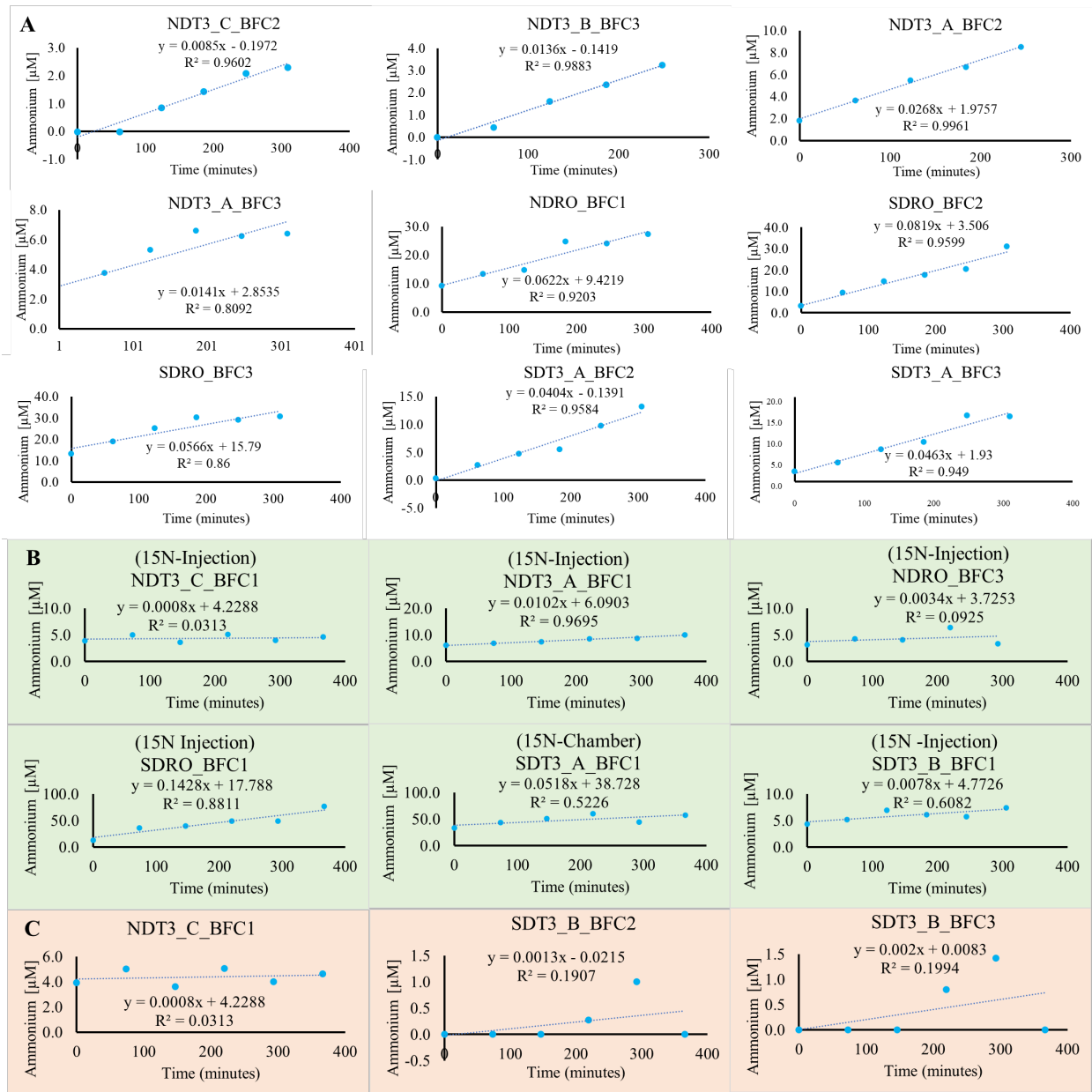
Supplemental Figure 1: A/white) Ammonium concentration changes over time from benthic flux chamber (BFC1, BFC2, BFC3) incubations. B/green) Ammonium concentration changes over time from ^{15}N-Nitrate benthic flux chamber incubations. Note these chambers were not used to calculate benthic fluxes. C/red) Ammonium concentration changes over time from benthic flux chamber incubations where there was no calculatable flux. No data are shown from chambers if there was a mechanical failure with the deployment or ammonium concentrations were all below detection. For station abbreviation definitions please refer to the main manuscript.
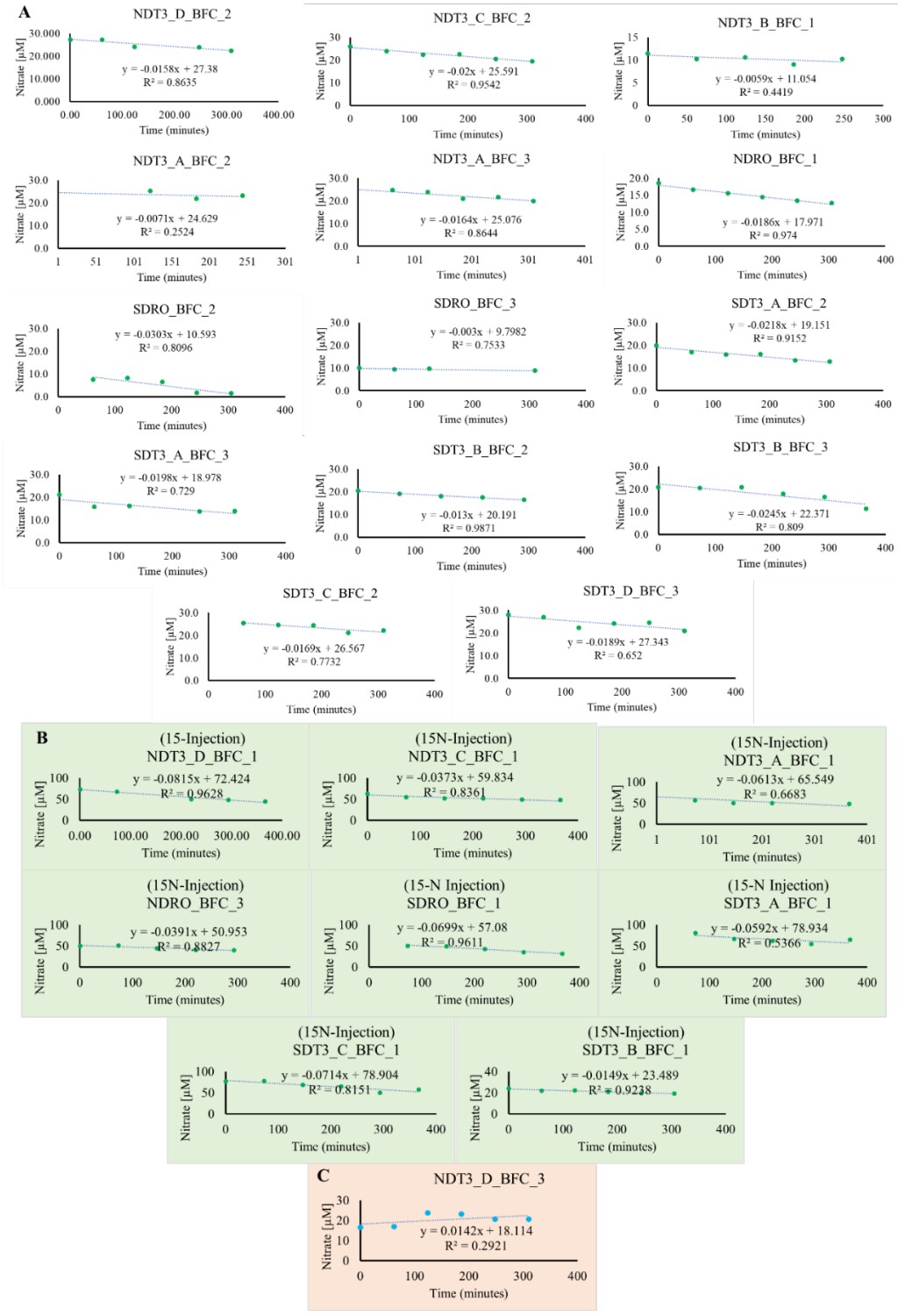
Supplemental Figure 2: A/white) Nitrate concentration changes over time from benthic flux chamber (BFC1, BFC2, BFC3) incubations. B/green) Nitrate concentration changes over time from ^{15}N-Nitrate benthic flux chamber incubations. Note these chambers were not used to calculate benthic fluxes. C/red) Nitrate concentration changes over time from benthic flux chamber incubations where there was no calculatable flux. No data are shown from chambers if there was a mechanical failure with the deployment. For station abbreviation definitions please refer to the main manuscript.
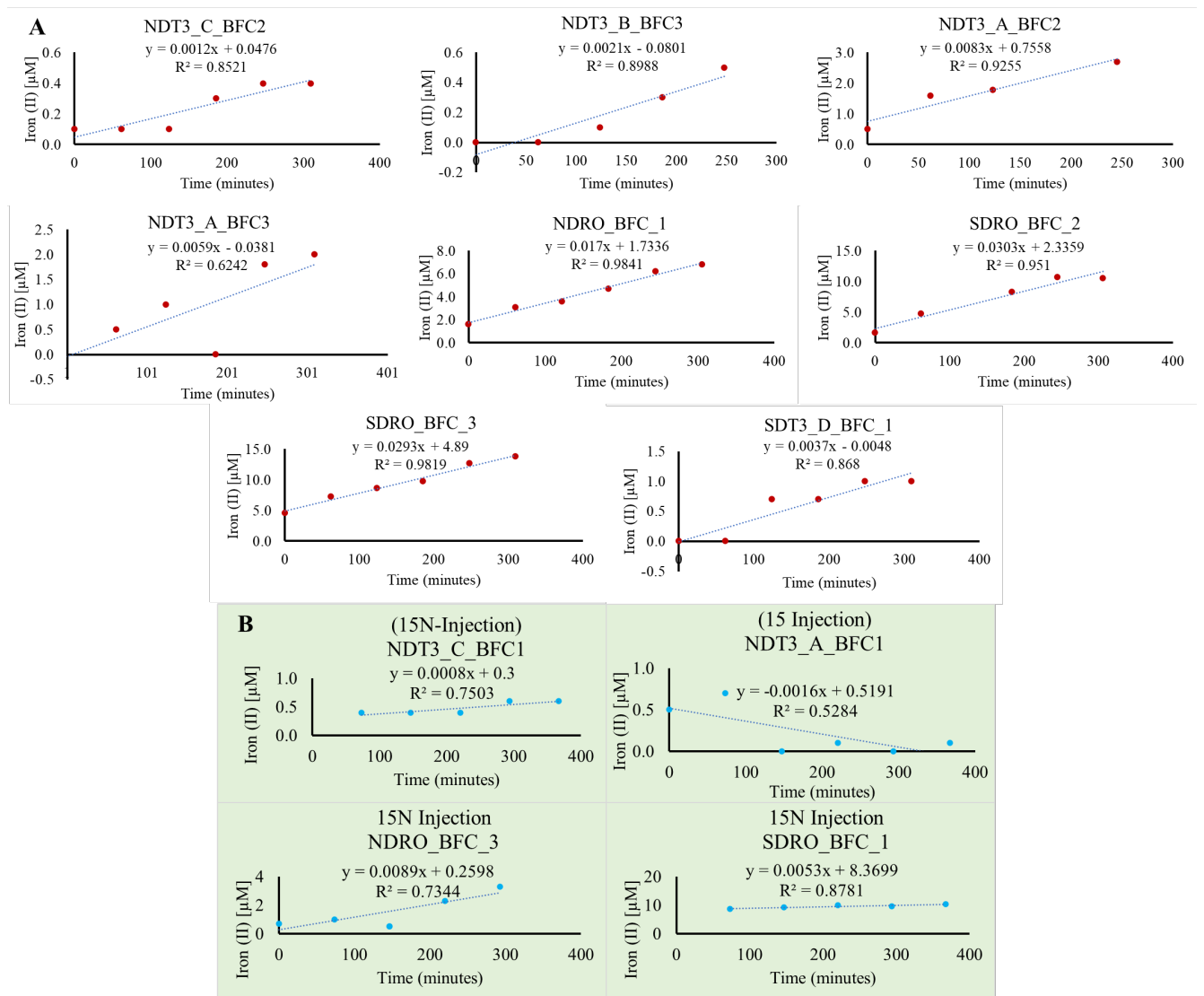
Supplemental Figure 3: A/white) Iron (II) concentration changes over time from benthic flux chamber (BFC1, BFC2, BFC3) incubations. B/green) Iron (II) concentration changes over time from ^{15}N-Nitrate benthic flux chamber incubations. Note these chambers were not used to calculate benthic fluxes. No data are shown from chambers if there was a mechanical failure with the deployment or concentrations were all below detection. For station abbreviation definitions please refer to the main manuscript.
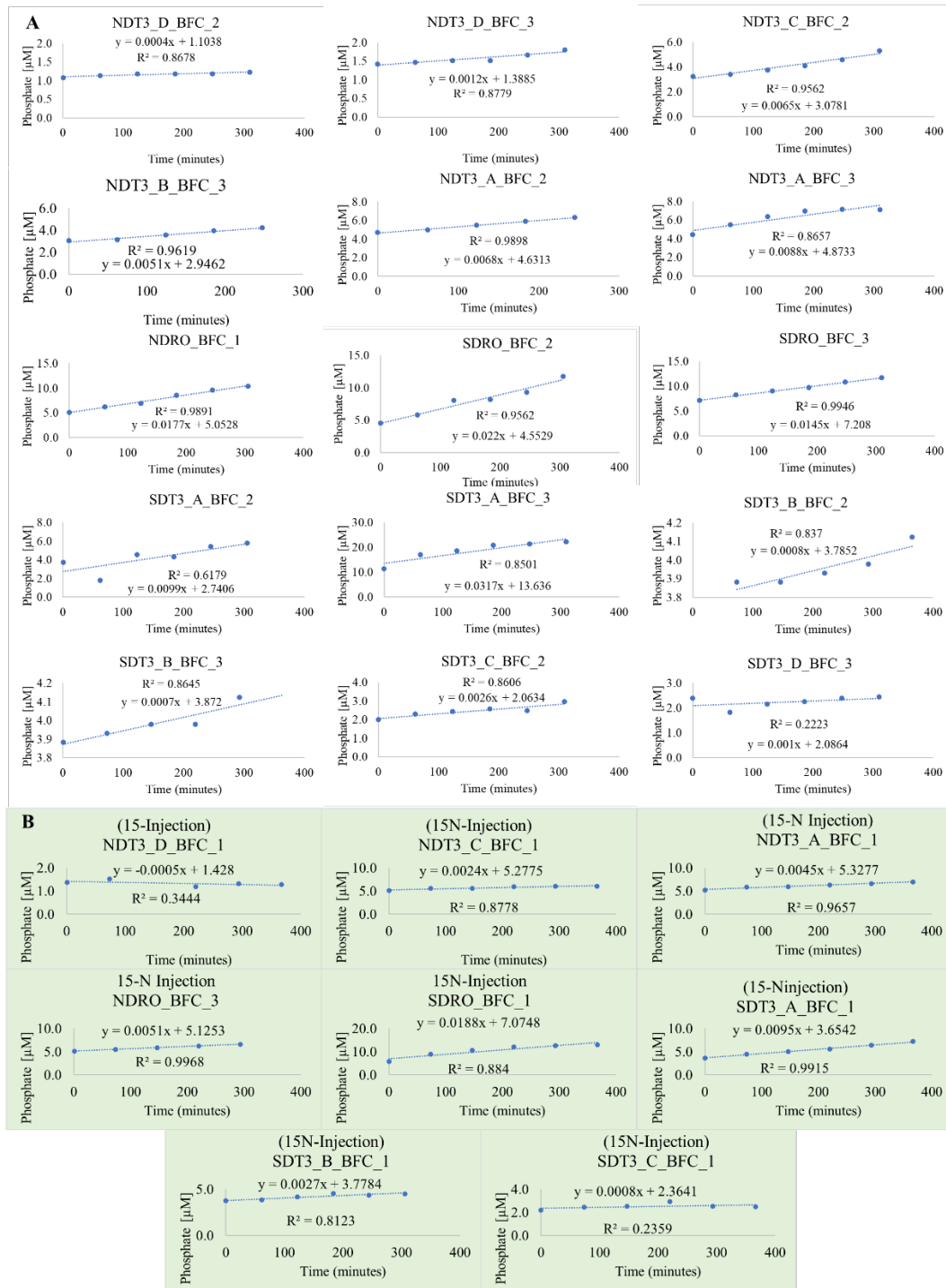
Supplemental Figure 4: A/white) Phosphate concentration changes over time from benthic flux chamber (BFC1, BFC2, BFC3) incubations. B/green) Phosphate concentration changes over time from ^{15}N-Nitrate benthic flux chamber incubations. Note these chambers were not used to calculate benthic fluxes. No data are shown from chambers if there was a mechanical failure with the deployment or concentrations were all below detection. For station abbreviation definitions please refer to the main manuscript.
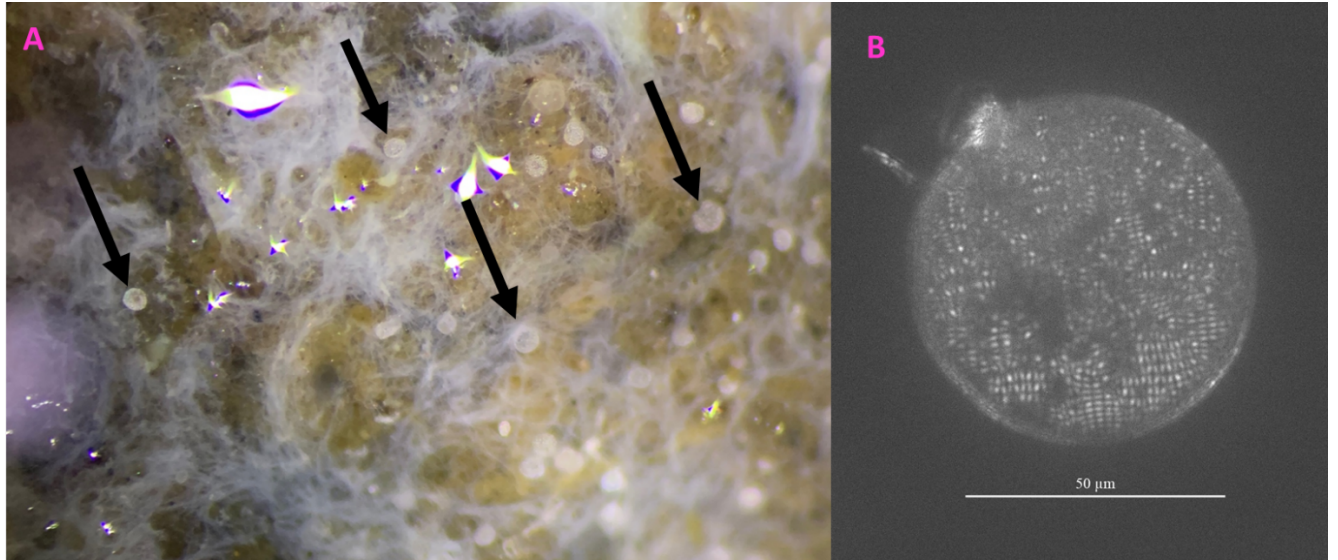
Supplementary Figure 5. A) Photograph of spherical sulfur bacteria mats (nicknamed 'ghost balls') within a mat of filamentous sulfur bacteria as seen through a dissection microscope. Black arrows point to a few of the ghost balls. B) Light Microscopy image of representative ghost ball with a scale bar. Ghost Balls were sampled from the 0-1 cm section of a core collected from station NDRO. The size of the ghost ball radius ranges between approx. 24.0 – 49.8 µm (n = 8).